Kinetics and Product of Ferrous Iron Oxygenation in Aqueous Systems

Windsor Sung* and James J. Morgan

W. M. Keck Laboratory of Environmental Engineering Science, California Institute of Technology, Pasadena, Calif. 91125

Iron is the fourth most abundant element by weight in the earth's crust. The chemistry of aqueous iron primarily involves the ferrous (II) and ferric (III) oxidation states and is of interest in water supplies, wastewaters, limnology, and oceanography. Recent quantitative studies have included: iron removal mechanisms in estuarine and oceanic waters (*1–3*); adsorption of trace metals by hydrous ferric oxides or ferric oxyhydroxides (*4–6*); iron speciation and redox reactions in synthetic and real seawater (*7–10*).

Although the oxygenation kinetics of ferrous iron have been studied extensively there is a rather wide spread in the reported rate constant. The present work was undertaken to study the effect of ionic media, alkalinity, and temperature on the kinetics of ferrous iron oxygenation and to identify the product(s) of oxygenation.

Methods

Iron Analysis. Ferrous iron concentration was determined spectrophotometrically with 1,10-phenanthroline, using fluoride as a masking agent for ferric iron (*11*). Ten-milliliter samples were quenched in 1 mL of 3.6 M sulfuric acid; 2 mL of 2 M ammonium fluoride, 1 mL of 1% 1,10-phenanthroline,

0013-936X/80/0914-0561$01.00/0

■ The oxygenation kinetics of ferrous iron in aqueous media were studied experimentally. Solutions buffered by HCO_3^- and CO_2 with $NaClO_4$, NaCl, and Na_2SO_4 were investigated. The general rate law was confirmed to be $-d[Fe(II)]/dt = k[OH^-]^2P_{O_2}[Fe(II)]$ for solutions with pH less than 7. The variation of the reported values of k with different alkalinities can be explained by the variation in ionic strength and temperature. The presence of NaCl and Na_2SO_4 reduces the rate further and adequately explains the observed rate in seawater, which is usually a factor of 100 times slower compared to solutions of freshwater-like composition. Autocatalysis of ferrous iron oxygenation was observed for pH greater than 7; a mathematical treatment of the kinetic data for this regime is presented. The product of oxygenation in various solution compositions was shown to be lepidocrocite, γ-FeOOH, by infrared spectroscopy and this was confirmed by X-ray diffraction.

and 5 mL of 2 M hexamethylenetetramine were added in that order, swirling the solution after the addition of each reagent. The solution was diluted with doubly distilled water to 25 mL, and the absorbance was measured at 510 nm. Five-centimeter cells were used with a Beckman Acta CIII spectrophotometer. Beer's law was obeyed with ferrous iron concentration as high as 7 mg/L = 125.3 μM and ferric iron background as high as 2500 mg/L = 44.76 mM. The molar absorptivity at 510 nm was determined to be 1.05×10^4 M^{-1} cm^{-1} with an accuracy of better than 1%.

Oxygenation Experiments. The water used for the experiments was doubly distilled and all chemicals used were analyzed reagent grade. The ferrous iron solutions were prepared by dissolving electrolyte grade iron powder in 0.1 M redistilled $HClO_4$. Bicarbonate–carbon dioxide buffers were prepared from solutions of sodium bicarbonate and bubbling through an air–CO_2 mixture. The air–CO_2 compressed gas mixtures were prepared and analyzed by Matheson Gas Co., Cucamonga, Calif. The test solutions were well thermostated (±0.1 °C) and vigorously stirred by a Teflon-coated magnetic stirrer. The pH was monitored continuously with a Beckman glass electrode and an Orion double junction reference electrode via an Orion 801A pH meter.

The $NaHCO_3$–NaX solution was added to a 1-L borosilicate glass beaker with a water jacket. The air–CO_2 mixture was bubbled through the stirred solution. When sufficient time had elapsed for the pH and temperature to reach equilibrium, the ferrous iron solution was added and a stopwatch started. Aliquots of the test solution were withdrawn at appropriate time intervals and analyzed for ferrous iron.

Standard Ferric Oxyhydroxide Preparation. Burns and Burns (*12*) reported five synthetic allotrophs of the ferric oxyhydroxides, α-, β-, γ-, δ-, and ε-FeOOH, and an additional amorphous ferric hydroxide. ε-FeOOH is a high-pressure polymorph and is not considered here. δ-FeOOH also was not considered since its natural occurrence is debatable.

Goethite, α-FeOOH, was obtained by hydrolyzing ferric nitrate in KOH (Fe/OH ratio = 0.25, final pH near 12) at 60 °C for 48 h. (See ref *13*.) At higher temperatures α-Fe_2O_3, hematite, forms. (Standard α-FeOOH was also obtained from Dr. G. R. Rossman of the Department of Geology, California Institute of Technology.) β-FeOOH, akaganeite, was obtained by hydrolyzing ferric chloride in HCl (Fe/H ratio = 9, final pH near 2) at 100 °C for 24 h. (See ref *14*.) γ-FeOOH, lepidocrocite, was obtained by oxidizing ferrous chloride in the presence of a slight excess of pyridine (final pH about 6) with air at room temperature for about 1 h. (Standard γ-FeOOH was also obtained from Dr. D. L. Janes of the 3M Co.)

The synthetic products were centrifuged, washed with distilled water three to four times, and dried at 45 °C in an oven.

Amorphous ferric hydroxide was obtained by hydrolyzing ferric nitrate in NaOH (Fe/OH ratio = 0.33, final pH near 8) at room temperature for 2 h. The product was filtered through a 0.22-μm Millipore filter and dried in a desiccator under slight vacuum. (A sample of amorphous iron oxyhydroxide was obtained from K. Hayes of Stanford University.)

Infrared Spectroscopy. At the conclusion of an oxygenation kinetics experiment, the solution was filtered through a 0.22-μm Millipore filter and the filter dried under slight vacuum in a desiccator. Appropriate amounts were scraped off with a spatula, dispersed in KBr powder, and pressed into a pellet (usually 1-mg sample in 200 mg of KBr). Infrared spectra were obtained for the 1400–200-cm^{-1} region with a Perkin-Elmer Model 180 spectrophotometer.

X-ray Diffraction. Oxygenation products were also placed in 0.3-mm glass capillary tubes and powder patterns obtained with a 114.6-mm Debye–Schrerrer camera with Co radiation and Fe filter. Typical exposure settings were 35 kV, 9 mA, and 16-h exposure time.

Results

Homogeneous Oxidation. The kinetics of ferrous iron oxygenation in laboratory systems have been previously studied (*10, 15–19*), and the general rate law was found to be:

$$-d[Fe(II)]/dt = k[OH^-]^2P_{O_2}[Fe(II)] \quad (1)$$

where k is the rate constant with units M^{-2} atm^{-1} min^{-1}, $[OH^-]$ denotes the concentration of hydroxyl ions, and [Fe(II)] denotes the concentration of total ferrous iron. At constant pH and P_{O_2}, Equation 1 reduces to a first-order equation:

$$-d[Fe(II)]/dt = k_1[Fe(II)] \quad (2)$$

where $k_1 = k[OH^-]^2P_{O_2}$ and has units of inverse time. Equation 2 integrates to:

$$[Fe(II)] = [Fe(II)]_0 \exp(-k_1t) \quad (3)$$

Pseudo-first-order kinetics with respect to ferrous iron were also observed in treatment plants or seawater (*3, 7, 20, 21*). Table I summarizes the reported values for k.

Since the rate is strongly dependent on pH, one of the major uncertainties in the numerical value for the rate constant arises from the variation of pH within an experiment. Reported variations range from ±0.02 to ±0.05 pH unit. Figure 1 shows the typical variation in pH during the course of an oxygenation experiment. The initial drop in pH coincides with the addition of the stock ferrous iron solution, which is also a source of strong-acid protons. The subsequent increase in pH can be adequately explained by the diffusion of aqueous CO_2 from the solution. Substantial error can be introduced if the oxygenation kinetics are studied on the same time scale of about 20 min. The variation of ferrous iron was plotted arithmetically vs. time and slopes were constructed to obtain instantaneous rates which were then normalized with respect to the instantaneous $[OH^-]$, P_{O_2}, and [Fe(II)] at that time. Rate constants obtained this way have about 20% variability (2σ) and compare well with the rate constants obtained by linear regression from first-order plots.

A series of experiments with ionic strength varying from 9×10^{-3} to 0.11 M was initiated at 25 °C. The results are summarized in Table II. Figure 2 shows the variation of log k with $\sqrt{I}$. Linear regression gives $\log k = 13.76 - 2.06\sqrt{I}$ with an r^2 of 0.97. When due regard was given to ionic strength dif-

Table I. Summary of Previous Results on Oxygenation Kinetics of Ferrous Iron

investigators	solution composition	reported rate information	remarks
Stumm and Lee (*15*)	29 to 39 mequiv/L of alk as $NaHCO_3$, P_{O_2} varies, T = 20.5 °C	$k = 8.0 \pm 2.5 \times 10^{13}$ M^{-2} atm^{-1} min^{-1}	assume ionic strength ≈ 34×10^{-3} M $\gamma_{OH} \approx 0.84$ K_H oxygen at 20.5 °C = 0.00138 M atm^{-1}
Morgan and Birkner (*16*)	P_{O_2} = 0.6 atm, T = 25 °C, alk = 32 mequiv/L	$\tau_{1/2} \approx$ 16 min at pH 6.70 → $k = 2.0 \times 10^{13}$ M^{-2} atm^{-1} min^{-1} $\tau_{1/2} \approx$ 47 min at pH 6.52 → $k = 1.7 \times 10^{13}$ M^{-2} atm^{-1} min^{-1}	
Schenk and Weber (*17*)	P_{O_2} = 0.21 atm, T = 25 °C, alk = 30–50 mequiv/L	$k = 2.1 \pm 0.5 \times 10^{13}$ M^{-2} atm^{-1} min^{-1}	assume ionic strength ≈ 40×10^{-3} M
Theis (*18*)	P_{O_2} = 0.5 atm, T = 25 °C, alk = 0.0158 M as NaOH initially	$\tau_{1/2}$ = 25.4 min at pH 6.3 → $k = 1.36 \times 10^{14}$ M^{-2} atm^{-1} min^{-1}	
Kester et al. (*7*)	T = ?, P_{O_2} = 0.21 atm, Naragansett seawater Sargasso seawater	$\tau_{1/2}$ = 5.5 min at pH 8.0 → $k = 6 \times 10^{11}$ M^{-2} atm^{-1} min^{-1} $\tau_{1/2}$ = 3.3 min at pH 8.0 → $k = 1 \times 10^{12}$ M^{-2} atm^{-1} min^{-1}	kinetics were followed by ferric iron absorbance in the UV region
Tamura et al. (*19*)	T = 25 °C, P_{O_2} varies, alk = 10^{-2} M $NaHCO_3$, total ionic strength = 0.11 M	0.1 M ClO_4^-: $k = 2.38 \times 10^{14}$ M^{-3} s^{-1} = 1.8×10^{13} M^{-2} atm^{-1} min^{-1} 0.1 M NO_3: $k = 2.04 \times 10^{14}$ M^{-3} s^{-1} = 1.6×10^{13} M^{-2} atm^{-1} min^{-1} 0.1 M Cl^-: $k = 1.63 \times 10^{14}$ M^{-3} s^{-1} = 2×10^{13} M^{-2} atm^{-1} min^{-1} 0.1 M Br^-, 0.1 M I^-, 0.033 M SO_4^{2-}: $k = 1.36 \times 10^{14}$ M^{-3} s^{-1} = 1.0×10^{13} M^{-2} atm^{-1} min^{-1}	
Murray and Gill (*3*)	T = ?, Puget Sound seawater	$\tau_{1/2}$ = 3.9 min at pH 8.0 → $k = 8.9 \times 10^{11}$ M^{-2} atm^{-1} min^{-1}	first 5 min linear on first-order plot

Table II. Variation of k with Ionic Strength (Adjusted by $NaClO_4$) [a]

ionic strength, M	$\tau_{1/2}$, min (least squares)	k, M^{-2} atm^{-1} min^{-1}
0.009	18.0	$4.0 \pm 0.6 \times 10^{13}$
0.012	18.2	$3.1 \pm 0.7 \times 10^{13}$
0.020	18.5	$2.9 \pm 0.6 \times 10^{13}$
0.040	21.5	$2.2 \pm 0.5 \times 10^{13}$
0.060	26.8	$1.8 \pm 0.3 \times 10^{13}$
0.110	37.9	$1.2 \pm 0.2 \times 10^{13}$

[a] T = 25 °C; alkalinity = 9×10^{-3} M $NaHCO_3$; $[Fe(II)]_0$ = 34.7 μM; P_{O_2} = 0.20 atm; pH ≈ 6.84.

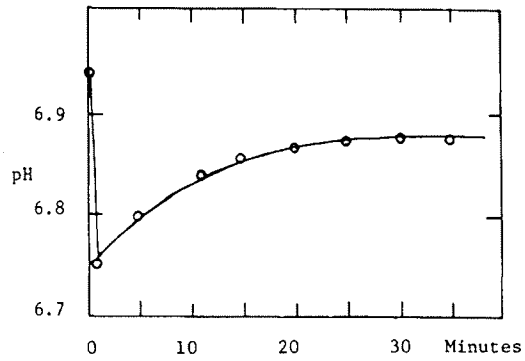

Figure 1. Variation of pH during an oxygenation experiment. Initial alkalinity = 10^{-2} M; P_{O_2} = 0.2 atm; P_{CO_2} = 0.071 atm; T = 25 °C. The initial drop in pH coincides with the addition of stock ferrous solution which introduces 1 mM protons

ferences, the rate constants of ref *16*, *17*, and *19* are in reasonable agreement with those found in this study. Better agreement with the data of ref *19* can be obtained if further normalization with respect to the activity coefficient of the OH^- ion is carried out. The value of Theis (*18*) is at variance with results in this study and no satisfactory explanation is evident.

Another series of experiments was initiated with temperature ranging from 5 to 30 °C. Figure 3 shows first-order plots for these experiments. The temperature effect appears to be large, but when normalization with respect to changes in K_w and O_2 solubility with temperature was carried out, as in Table III, the rate constant was seen to vary slightly with temperature. When proper attention was given to ionic strength, it was found that this study's results compare well with those of ref *15*. The error bars are sufficiently large to make meaningful calculations of activation energy impossible.

Tamura et al. (*19*) studied the effects of anions on the oxygenation kinetics of ferrous iron and found the rate constant to decrease in the order ClO_4^-, NO_3^-, Cl^-, Br^-, I^-, SO_4^{2-}. The present study confirms the order of ClO_4^-, Cl^-, and SO_4^{2-}. Figure 4 shows first-order plots of ferrous iron oxygenation in chloride media.

The role of alkalinity in the oxygenation kinetics is unclear, apart from its buffering capacity for acidity and its contribution to the ionic strength. Data from this study show that effects of variation in alkalinity from 9 to 50 mM can be adequately explained by ionic strength effects. Tamura et al. (*19*) reported that the rate constant did not change with variations of bicarbonate from 2 to 10 mM. The scatter in data is large for low alkalinities (less than 5 mM) and may result in spuriously high rate constants.

Tamura et al. (*19*) proposed the following reaction as the rate-limiting step: $FeOH^+ + O_2OH^- \rightarrow Fe(OH)_2^+ + O_2^-$. If this is correct, transition-state theory predicts a slope of −1 in a plot of log k vs. $\sqrt{I}$. Instead, the present study shows a slope of −2, which indicates that the product of the charges of the species involved in the rate-limiting step is −2.

Kester et al. (*7*) and Murray and Gill (*3*) reported $\tau_{1/2}$ of ferrous iron oxidation in seawater to be in the range of 3–6 min. Tamura et al. (*19*) studied the effects of anions on ferrous iron oxidation and proposed that complexation of ferrous iron by anions can account for retardation of oxygenation. From the data in Table IV (discussed under Heterogeneous Oxidation), it can be shown that, at pH 8, the $\tau_{1/2}$ of ferrous iron oxidation in 0.50 M NaCl or 0.165 M Na_2SO_4 is on the order of 1 min. This work confirms that of Liang and Kester (*10*)

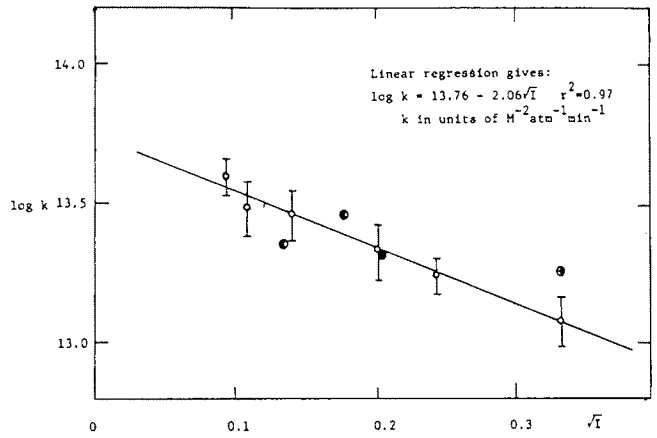

Figure 2. The effect of ionic strength on the rate constant of ferrous iron oxygenation. All experiments of this study are: T = 25 °C; P_{O_2} = 0.2 atm, alkalinity = 9 mM, and ionic strength adjusted by $NaClO_4$. (○) This study; (⊕) Tamura et al. (*19*); (◐) Morgan and Birkner (*16*); (●) Schenk and Weber (*17*).

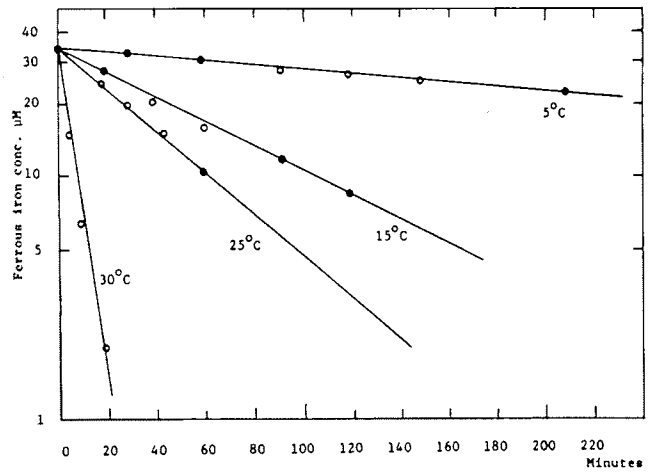

Figure 3. Effect of temperature on the oxygenation kinetics of ferrous iron. All experiments are conducted in 0.11 M ionic strength adjusted with $NaClO_4$; alkalinity = 9 mM as $NaHCO_3$; P_{O_2} = 0.2 atm; pH ~6.82; $[Fe(II)]_0$ = 34.7 μM

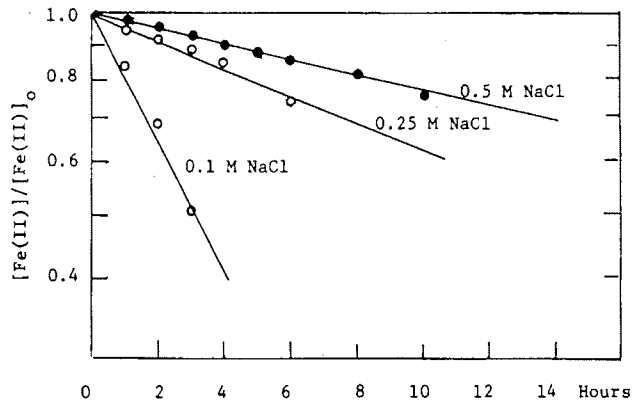

Figure 4. Effect of Cl^- anions on the oxygenation kinetics of ferrous iron: pH 6.50; P_{O_2} = 0.2 atm; T = 25 °C; alkalinity = 5 mM as $NaHCO_3$; $[Fe(II)]_0$ = 50 μM

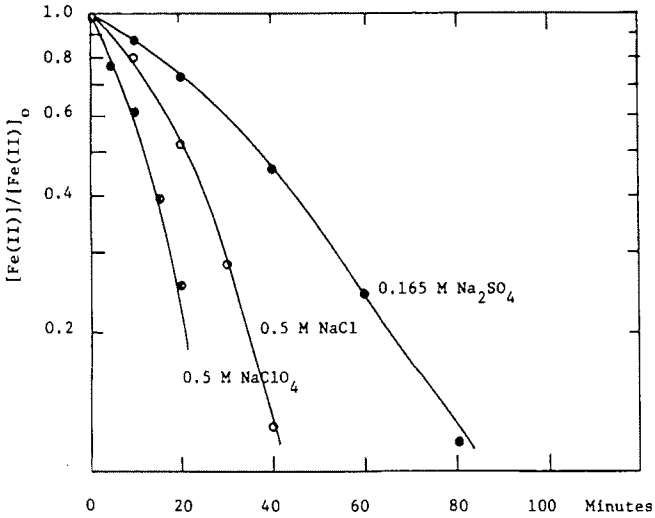

Figure 5. Effect of anions on the oxygenation kinetics of ferrous iron: pH 7.2; P_{O_2} = 0.2 atm; T = 25 °C; ionic strength = 0.5 M; alkalinity = 5 mM as $NaHCO_3$; $[Fe(II)]_0$ = 50 μM

that the presence of Cl^- and SO_4^{2-} anions can effectively reduce the oxygenation rate to that of its counterpart in seawater.

Heterogeneous Oxidation. Takai (*22*) studied the catalytic oxidation removal of Fe(II) by α-FeOOH and γ-FeOOH experimentally and found the latter to be effective. Tamura et al. (*23*) studied the effect of ferric hydroxide on the oxygenation of ferrous iron in neutral solutions and found that at constant pH and O_2 concentration the rate is:

$$-d[Fe(II)]/dt = (k_1 + k_2[Fe(III)])[Fe(II)] \quad (4)$$

where k_1 is the homogeneous rate constant with inverse time units and k_2 is the heterogeneous rate constant with inverse concentration and time units (M^{-1} min^{-1}). They also showed that:

$$k_2 = k_s[O_2]K/[H^+] \quad (5)$$

where k_s is the surface rate in M^{-1} min^{-1}, $[O_2]$ is the concentration of oxygen in solution, and K is the adsorption constant of ferrous iron on ferric hydroxide, whose numerical value was determined to be $10^{-9.6}$ mol mg^{-1} for amorphous iron hydroxide, which converts to the dimensionless value of $10^{-4.85}$.

For a system with ferric iron initially absent, we can write the mass balance for any time:

$$[Fe(III)] + [Fe(II)] \approx [Fe(II)]_0 \quad (6)$$

Substituting Equation 6 into 4, we obtain the autocatalytic rate law:

$$\frac{-d[Fe(II)]}{dt} = \{k_1 + k_2([Fe(II)]_0 - [Fe(II)])\}[Fe(II)]$$

$$= (k_1 + k_2[Fe(II)])_0[Fe(II)] - k_2[Fe(II)]^2 \quad (7)$$

This equation can be readily integrated for the condition at t = 0:

$$[Fe(II)] = [Fe(II)]_0$$

to give:

$$[Fe(II)] = \frac{[Fe(II)]_0(k_1 + k_2[Fe(II)]_0)}{k_2[Fe(II)]_0 + k_1 \exp[(k_1 + k_2[Fe(II)]_0)t]} \quad (8)$$

If $k_1 \gg k_2[Fe(II)]_0$, Equation 8 reduces to Equation 3:

$$[Fe(II)] \approx \frac{[Fe(II)]_0 k_1}{k_1 \exp[(k_1)t]} = [Fe(II)]_0 \exp(-k_1 t)$$

Using the reported values of Tamura et al. (*23*), k_2 (at pH 7, 25 °C, and a P_{O_2} of 0.21 atm) is 133.6 M^{-1} min^{-1} and $k_2[Fe(II)]_0 = 6.68 \times 10^{-3}$ min^{-1} for $[Fe(II)]_0$ = 50 μM. For the same conditions, k_1 is ~7.5×10^{-2} min^{-1} for 0.01 M ionic strength, so $k_1/k_2[Fe(II)]_0 \approx 11$. The ratio $k_1/k_2[Fe(II)]_0$ ac-

Table III. Variation of k with Temperature [a]

T, °C	$\tau_{1/2}$, min	pH	$K_W \times 10^{14}$	O_2 saturation $\times 10^4$ M	k, M^{-3} min^{-1}
5	315.6	6.76	0.1846	3.81	$2.7 \pm 0.5 \times 10^{16}$
15	63.1	6.80	0.4505	3.06	$2.2 \pm 0.3 \times 10^{16}$
20.5 [b]			0.70		
25	37.9	6.84	1.008	2.50	$9.4 \pm 1.7 \times 10^{15}$
30	4.1	6.88	1.469	2.28	$3.3 \pm 0.7 \times 10^{16}$

[a] Alkalinity = 9×10^{-3} M $NaHCO_3$; ionic strength = 0.11 M adjusted by $NaClO_4$; P_{O_2} = 0.20 atm; $[Fe(II)]_0$ = 34.7 μM. [b] Stumm and Lee (*15*). $k = 8.0 \pm 2.5 \times 10^{13}$ M^{-2} atm^{-1} min^{-1}. $k = 5.8 \pm 1.8 \times 10^{16}$ M^{-3} min^{-1} at 34 mM ionic strength. $k = 2.9 \pm 0.9 \times 10^{16}$ M^{-3} min^{-1} at 0.11 M ionic strength using the −2 slope dependence of log k on $\sqrt{I}$.

Table IV. Values of k_1 and k_2 in Autocatalytic Rate Expression

solution composition [b]	pH	$\tau_{1/2}$	$K_C W \times 10^{14}$ [a]	k_1, min^{-1}	k, M^{-2} atm^{-1} min^{-1}	k_2, M^{-1} min^{-1}
0.1 M NaCl	6.5	3.108 h	13.803	0.037 717	8.8×10^{12}	
0.25 M NaCl	6.5	13.577 h	13.82	0.000 8509	1.9×10^{12}	
0.50 M NaCl	6.5	22.8 44 h	13.864	0.000 5057	1.6×10^{12}	
0.50 M $NaClO_4$	7.2	≈12 min	13.86	0.056	5.6×10^{12}	360
0.50 M NaCl	7.2	≈21 min	13.86	0.018	1.8×10^{12}	1440
0.165 M Na_2SO_4	7.2	≈36 min	13.86	0.016	7.8×10^{11}	360
0.70 M NaCl, alk = 2.5×10^{-3} M	7.05		13.926	0.0079	2.1×10^{12}	365

[a] $K_C W$ is the concentration quotient $[H^+][OH^-]$ calculated from equation (4-34), log $K_C W$ = log k + $[aI^{1/2}(1 + I^{1/2})] + bI$, of Baes and Mesmer (*28*). Note: Tamura et al. (*23*) derived $k_2 = k_s[O_2]K/[H^+]$ for pH 6–7, $[Fe(III)]_0$ = 30 mg/L, ionic strength 0.11 M. k_s = 4380 M^{-1} min^{-1}, $K = 10^{-9.6}$ mol/mg = $10^{-4.85}$ at pH 7.2, $[O_2] = 2.2 \times 10^{-4}$ M for 0.5 M NaCl, $k_2 \approx (4380\ M^{-1}\ min^{-1} \times 2.2 \times 10^{-4}\ M \times 10^{-4.85})/10^{-7.2}\ M = 212\ M^{-1}\ min^{-1}$. [b] Alkalinity = 5×10^{-3} M; unless stated otherwise, 25 °C.

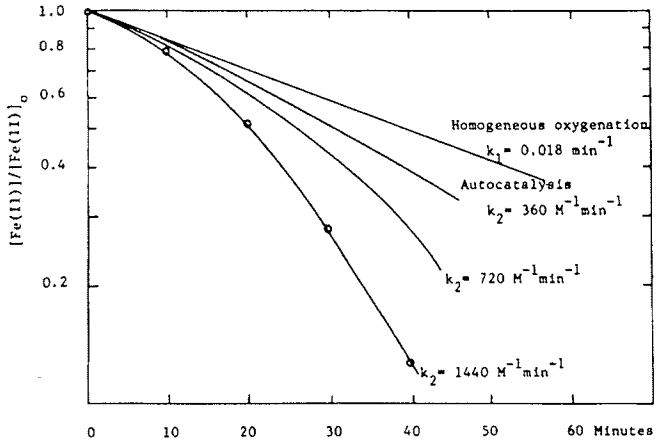

Figure 6. Modelling of autocatalytic oxygenation of ferrous iron with Equation 8 of text. Experimental conditions: 0.5 M NaCl; pH 7.2; P_{O_2} = 0.2 atm; T = 25 °C; alkalinity = 5 mM as $NaHCO_3$; $[Fe(II)]_0$ = 50 μM

tually decreases with decreasing pH since k_1 has a square dependence on $[OH^-]$, while k_2 is directly proportional to $[OH^-]$. But at lower pH values, the surface forms slowly and adsorption of ferrous iron is less favorable. As a result, autocatalysis is noticeable only for pH around 7 and above.

Figure 5 shows the oxygenation of ferrous iron in ClO_4^-, Cl^-, and SO_4^{2-} media at pH 7.2. There are two ways to obtain the rate constant k_2. We can first get the homogeneous rate constant k at lower pH values and use the $[OH^-]^2$ dependence to obtain the suitable k_1 at that pH. Then k_2 can be adjusted until a good fit is obtained between predicted values by Equation 8 and the experimental data. This procedure is shown in Figure 6. Alternatively, we can utilize plots of log $\{([Fe(II)]_0 - [Fe(II)]) + k_1/k_2\}/[Fe(II)]$ vs. time. Assuming, in a first trial, that k_1/k_2 is small and plotting log $([Fe(II)]_0 - [Fe(II)])/[Fe(II)]$, the straight line will have a slope of $(k_1 + k_2[Fe(II)]_0)/2.303$ and an intercept of log $k_1/(k_2[Fe(II)]_0)$. The values for k_1 and k_2 thus obtained can be substituted in a second trial and the log function plotted again. A convergence in k_1/k_2 is obtained in a few trials. Pertinent data are summarized in Table IV. The agreement between Tamura et al. (*23*) and this study is surprisingly good, since their adsorption constant K was obtained for amorphous iron hydroxide formed by hydrolysis and not oxygenation.

Table V. X-ray Diffraction Pattern of Fe(II) Oxygenation Product

d, Å	Intensity	d, Å	Intensity	d [a]	I/I_0 [a]
6.36	s, br	2.380	ww	6.26	100
3.27	s	1.996	m, sh	3.29	90
2.821	ms, sh	1.9385	s	2.47	80
2.479	br, s	1.5297	w, br		

[a] The three strongest lines of lepidocrocite from ASTM card file 8-98.

Product Identification. Initial attempts to obtain X-ray diffraction patterns for the oxygenation products were unsuccessful. They were amorphous to X-rays. Misawa et al. (*24*) claimed that γ-FeOOH was formed in cases of the rapid aerial oxidation of ferrous iron and Fe(II)–Fe(III) green intermediates in neutral and slightly acidic solutions. In order to gain information about the nature of the products, additional experimental techniques were needed. Infrared spectroscopy turned out to be most useful in this case. Standard infrared spectra for various ferric oxyhydroxides have been reported (*22, 25–27*), but their spectra were not very useful for purposes of this investigation. Figure 7 shows the standard spectra compiled for this study. When the infrared spectra of the oxygenation products in Figure 8 were compared with the standard patterns, it was readily apparent that the product had an infrared spectra closest to the γ-FeOOH pattern. Some of the oxygenation products gave recognizable X-ray diffraction patterns (tabulated in Table V) confirming that γ-FeOOH is the product.

Figure 9 shows the spectra of some products formed by hydrolyzing ferric salts. Amorphous ferric hydroxide is formed at slightly alkaline pH values, even when Cl^- is present. Apparently, the formation of β-FeOOH is an aging process and

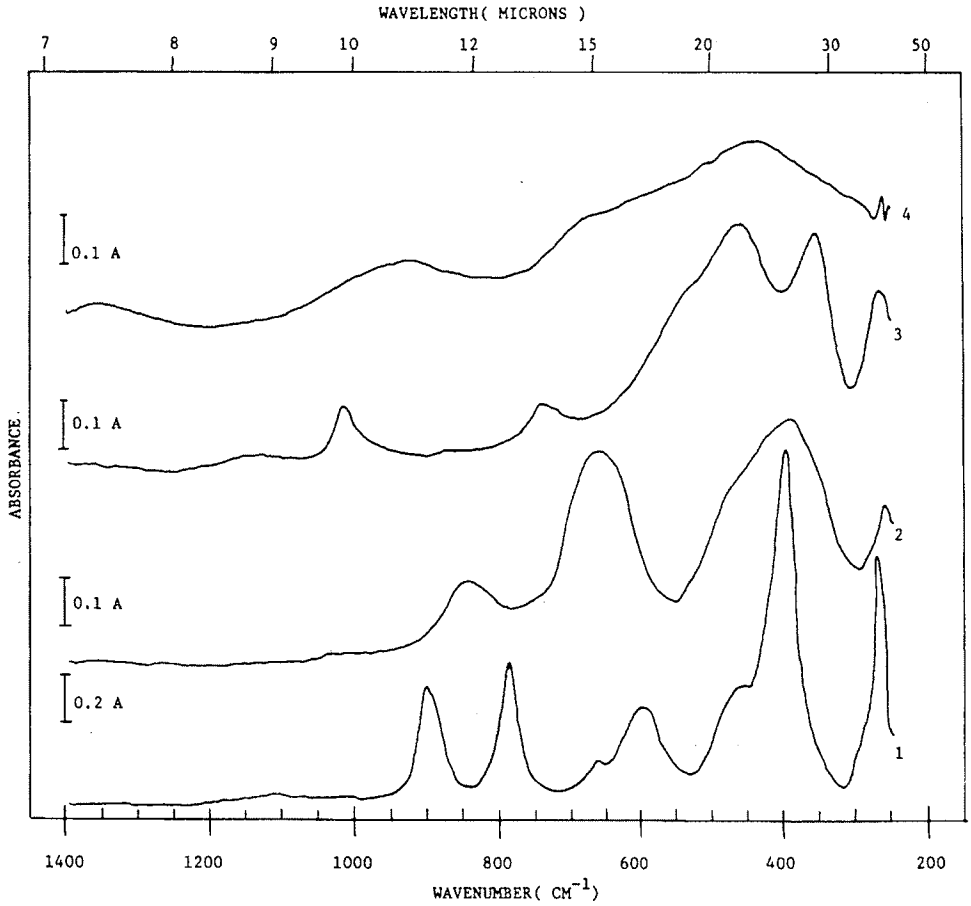

Figure 7. Infrared spectra of standard ferric oxyhydroxides: (1) α-FeOOH, synthetic; obtained from G. Rossman, California Institute of Technology, 0.8-mg sample in 2.00 mg of KBr. (2) β-FeOOH, synthetic; 1-mg sample in 200 mg of KBr. (3) γ-FeOOH, synthetic; 0.6-mg sample in 200 mg of KBr. (4) Amorphous FeOOH, synthetic; 1-mg sample in 200 mg of KBr

requires a time scale much longer than hours at such pH values. The hydrolyzed ferric oxide at pH values close to 12 exhibits goethite peaks, although X-ray diffraction shows it to be amorphous. It is of interest to note that, although it is known that anions are important in determining the nature of the product in ferric salt hydrolysis, in oxygenation experiments it is γ-FeOOH that invariably forms first, whether ClO_4^-, Cl^-, or SO_4^{2-} media. The γ-FeOOH so formed is unstable, as γ-FeOOH is unstable with respect to α-FeOOH.

Summary and Conclusions

This work presents new experimental data on the oxygenation kinetics of ferrous iron in aqueous systems and on the identity of the solid phase formed in the reaction. We have attempted to place these results and earlier observations for the oxygenation process in a consistent framework to help to account for the behavior of iron in different aquatic environments.

The general rate law, consistent with earlier work, is:

$$-\frac{d[Fe(II)]}{dt} = k[OH^-]^2P_{O_2}[Fe(II)] = k'[OH^-]^2[O_2][Fe(II)]$$

where k' is related to k by the Henry's law constant for oxygen and the activity coefficient of oxygen. For solutions of sufficiently low pH, ca. 7, the rate constant k is dependent on ionic strength, concentration of individual anions, and temperature. At 25 °C, pH 6.84, and P_{O_2} = 0.20 atm, an increase of ionic strength (with $NaClO_4$) from 9 to 110 mM increases the half-time for oxidation from 18 to 38 min. A change in temperature from 5 to 30 °C (P_{O_2} = 0.20 atm, pH 6.84, ionic strength = 110 mM, alkalinity = 9 mequiv/L) causes a decrease in oxidation half-time from 316 to 4 min, which is mainly caused by the change in OH^- concentration due to the temperature dependence of the ionization constant of water.

Chloride and sulfate ions have a significant retarding influence on the oxygenation rate in the pH range from 6.5 to 7.2. The oxygenation half-times are in the sequence $SO_4^{2-} > Cl^- > ClO_4^-$ for constant ionic strength in agreement with the results of Tamura et al. (*19*).

For pH greater than ~7, the kinetic data indicate catalysis of aqueous Fe(II) disappearance by the reaction product. An autocatalytic rate expression with first- and second-order rate constants k_1 and k_2, where k_1 is the apparent homogeneous rate constant and k_2 the apparent catalytic constant, adequately describes the experimental data.

Comparison of the infrared (IR) spectra of products of our oxygenation experiments under various solution conditions with IR spectra of ferric oxyhydroxide standards showed that the product was invariably closest to γ-FeOOH, lepidocrocite. This observation was confirmed by comparison of the X-ray diffraction patterns of the Fe(II) oxygenation product with that of standard lepidocrocite.

The results of this study may have implications for understanding the short-term dynamics of iron transformations in freshwater and marine systems. It is suggested that an autocatalytic rate expression is needed at higher pH, and that the influence of simple media ions (Cl^-, SO_4^{2-}) in retarding oxygenation–removal helps to explain reported differences in behavior for freshwater, estuarine, and marine waters. An Fe(II) oxygenation half-time on the order of minutes, rather than seconds, for marine waters may help to provide an explanation for biological availabilities of Fe(II) and Fe(III) in

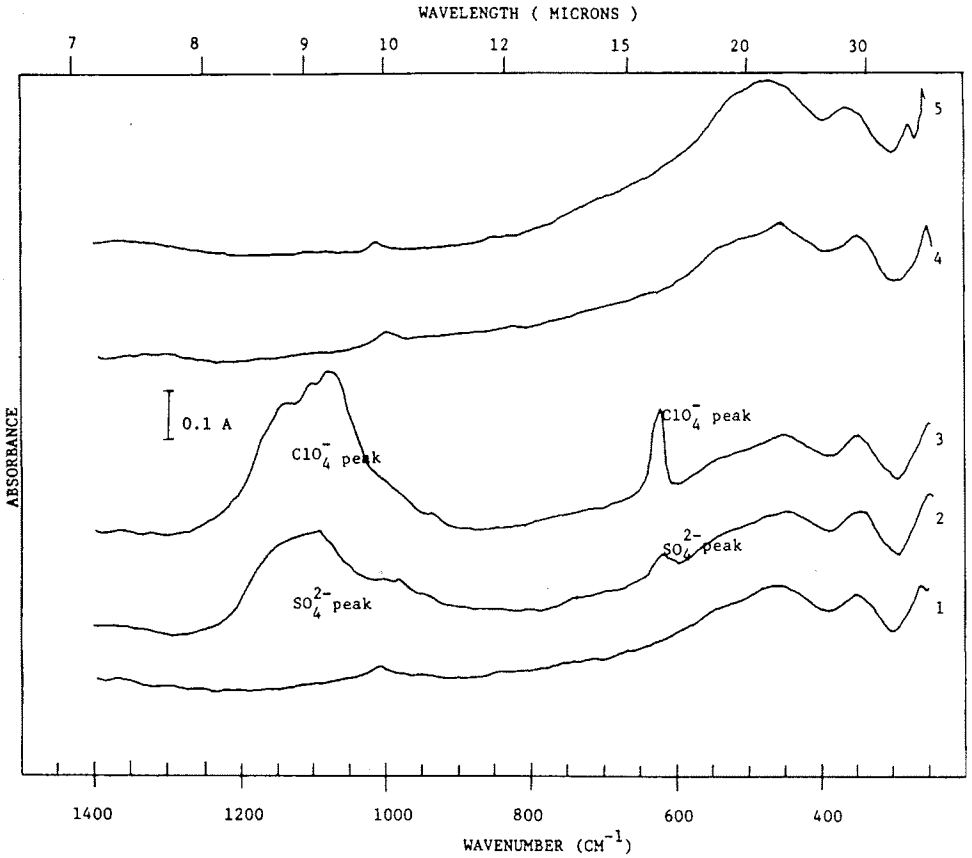

Figure 8. Infrared spectra of ferrous iron oxygenation product. All spectra run with 1-mg sample in 200 mg of KBr. Spectra 1, 2, and 3 are run at experimental conditions of pH 7.2, $T = 25$ °C, ionic strength = 0.5 M, HCO_3^-/CO_2 buffers, $[Fe(II)]_0 = 50$ μM: (1) 0.5 M NaCl; (2) 0.165 M Na_2SO_4; (3) 0.5 M $NaClO_4$; (4) experimental conditions—pH 8.3, $T = 25$ °C, 0.7 M NaCl, HCO_3^-/CO_2 buffers, $[Fe(II)]_0 = 10^{-3}$ M; (5) experimental conditions—pH 9.0, $T = 25$ °C, 0.1 M $NaClO_4$, NH_4^+/NH_3 buffers

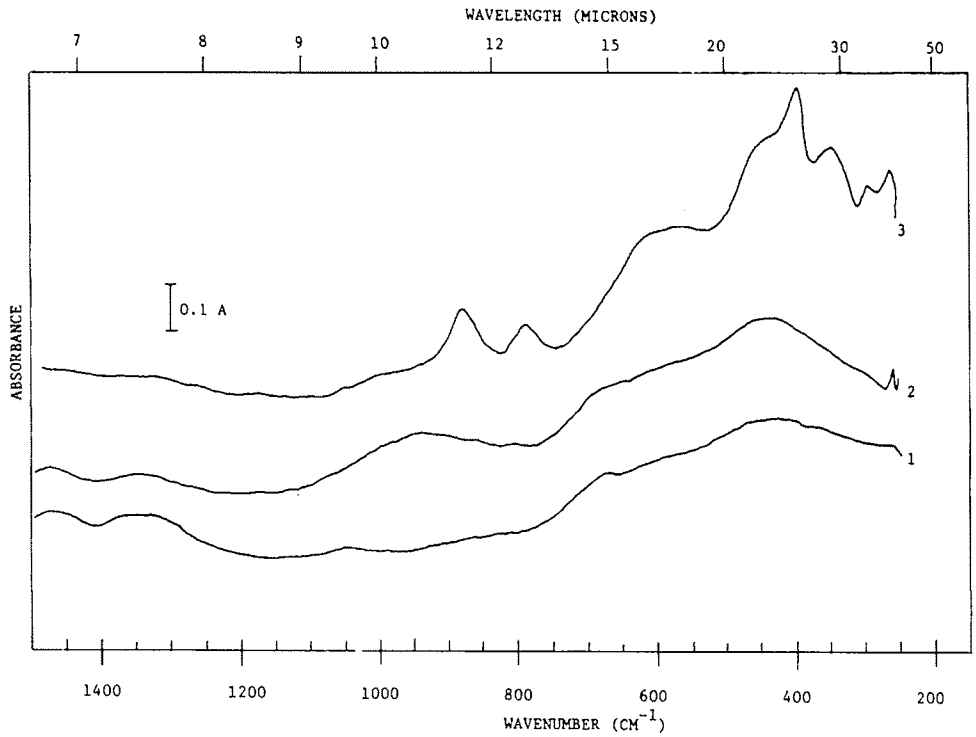

Figure 9. Infrared spectra of some ferric iron hydrolysis products. All spectra run with 1-mg sample in 200 mg of KBr: (1) 10^{-3} M $Fe(ClO_4)_3$ in 0.7 M NaCl; pH 8.3 by HCO_3^-/CO_2 buffer; 4-h equilibration time. (2) $Fe(NO_3)_3$ in 0.1 M $NaNO_3$; pH 8 by addition of CO_3^{2-} free NaOH; from K. Hayes, Stanford University. (3) $FeCl_3$ in 0.01 M NaOH; from D. Wilson, Waterways Experimental Station, Vicksburg, Miss.

surface waters containing both reducing agents and dissolved oxygen. The observation that γ-FeOOH is the oxygenation product under the solution conditions studied suggests that this ferric oxyhydroxide adsorbent merits study in work on adsorption directed to natural waters. In the long run, γ-FeOOH is unstable with respect to α-FeOOH, but short-term sorption and catalytic behavior will be governed by the nature of the immediate oxygenation products.

Literature Cited

(1) Sholkovitz, E. R., *Geochim. Cosmochim. Acta*, **40**, 831–45 (1976).
(2) Boyle, E. A., Edmond, J. M., Sholkovitz, E. R., *Geochim. Cosmochim. Acta*, **41**, 1313–24 (1977).
(3) Murray, J. W., Gill, G., *Geochim. Cosmochim. Acta*, **42**, 9–19 (1978).
(4) Gadde, R. R., Laitinen, H. A., *Anal. Chem.*, **46**, 2022–6 (1974).
(5) Swallow, K. C., Ph.D. Dissertation, Massachusetts Institute of Technology, Cambridge, Mass., 1978.
(6) Davies, J. A., Leckie, J. O., *J. Colloid Interface Sci.*, **67**, 90–107 (1978).
(7) Kester, D. A., Byrne, R. H., Liang, Y. J., "Marine Chemistry in the Coastal Environment", Church, T. M., Ed., ACS Symposium Series No. 18, Philadelphia, Penn., April 8–10, 1975, Chapter 3.
(8) Byrne, R. H., Kester, D. R., *Mar. Chem.*, **4**, 255–74 (1976).
(9) Byrne, R. H., Kester, D. R., *Mar. Chem.*, **4**, 275–87 (1976).
(10) Liang, Y. J., Kester, D. R., *Eos Trans. AGU*, **58**, 1168 (1977).
(11) Tamura, H., Goto, K., Yotsuyanagi, T., Nagayama, M., *Talanta*, **21**, 314–8 (1974).
(12) Burns, R. G., Burns, V. M., "Marine Manganese Nodules", Glasby, G. P., Ed., Elsevier, New York, 1977, Chapter 7.
(13) Atkinson, R. J., Posner, A. M., Quirk, J. P., *J. Phys. Chem.*, **71**, 550–8 (67).
(14) Matijevic, E., Scheiver, P., *J. Colloid Interface Sci.*, **63**, 509–24 (1978).
(15) Stumm, W., Lee, G. F., *Ind. Eng. Chem.*, **53**, 143–6 (1961).
(16) Morgan, J. J., Birkner, F. B., *J. San. Eng. Div., Proc. Am. Soc. Civ. Eng.*, **16**, SA6, 137–43 (1966).
(17) Schenk, J. E., Weber, Jr., W. J., *J. Am. Water Works Assoc.*, **60**, 199–212 (1968).
(18) Theis, T. L., Ph.D. Dissertation, Notre Dame University, Notre Dame, Ind., 1972.
(19) Tamura, H., Goto, K., Nagayama, M., *J. Inorg. Nucl. Chem.*, **38**, 113–7 (1976).
(20) Ghosh, M. M., O'Connor, J. T., Engelbrecht, R. S., *J. San. Eng. Div., Proc. Am. Soc. Civ. Eng.*, **16**, SAI, 199–213 (1966).
(21) Larson, T. E., "Principles and Applications of Water Chemistry", Faust, S. D., Hunter, J. V., Ed., Wiley, New York, 1967.
(22) Takai, T., *J. Jpn. Water Works Assoc.*, **466**, 22–33 (1973).
(23) Tamura, H., Goto, K., Nagayama, M., *Corros. Sci.*, **16**, 197–207 (1976).
(24) Misawa, T., Hashimoto, K., Shimodaira, S., *Corros. Sci.*, **14**, 131–49 (1974).
(25) Landa, E. R., Gast, R. G., *Clays Clay Min.*, **21**, 121–30 (1973).
(26) Powers, D. A., Ph.D. Dissertation, California Institute of Technology, Pasadena, 1975.
(27) Kauffman, K., Hazel, F., *J. Inorg. Nucl. Chem.*, **37**, 1139–48 (1975).
(28) Baes, C. F., Mesmer, R. E., "The Hydrolysis of Cations", Wiley, New York, 1976, Chapter 4.

Received for review October 1, 1979. Accepted February 1, 1980. This work was supported in part by grants from the Union Oil Company of California and the Du Pont Corporation. Based on a paper presented at the 177th National Meeting of the American Chemical Society, Honolulu, Hawaii, April 1–6, 1979, Division of Environmental Chemistry.